Int. J. Metrol. Qual. Eng. **7**, 401 (2016)

DOI: 10.1051/ijmqe/2016021

Available online at:
www.metrology-journal.org

Control chart limits based on true process capability with consideration of measurement system error

Souha Ben Amara[1,2,*], Jamel Dhahri[1], and Nabil Ben Fredj[1]

[1] Laboratoire de Mécanique, Matériaux et Procédés (LR99ES05), ENSIT, University of Tunis, 5 Av Taha Hussein Montfleury, 1008 Tunis, Tunisia
[2] ENIM, University of Monastir, Av Ibn Eljazzar, 5019 Monastir, Tunisia

Received: 11 April 2016 / Accepted: 16 September 2016

Abstract. Shewhart $\overline{X}$ and R control charts and process capability indices, proven to be effective tools in statistical process control are widely used under the assumption that the measurement system is free from errors. However, measurement variability is unavoidable and may be evaluated by the measurement system discrimination ratio (DR). This paper investigates the effects of measurement system variability evaluated by DR on the process capability indices C_p and C_{pm}, on the expected non conforming units of product per million (ppm), on the expected mean value of the Taguchi loss function (E(Loss)) and on the Shewhart charts properties. It is shown that when measurement system variability is neglected, an overestimation of ppm and underestimation of E(Loss) are induced. Moreover, significant effects of the measurement variability on the control chart properties were made in evidence. Therefore, control charts limits calculation methods based on process real state were developed. An example is provided in order to compare the proposed limits with those traditionally calculated for Shewhart $\overline{X}$, R charts.

Keywords: process capability indices / expected non conforming units of product per million (ppm) / mean value of Taguchi loss function E(Loss) / measurement system discrimination ratio / Shewhart $\overline{X}$, R control chart parameters

1 Introduction

Quality is actually an ongoing challenge facing manufacturing industry. Hence, manufacturers have resorted to statistical process control (SPC) for monitoring, maintaining and improving the performance of process to produce parts conforming to their customer's expectations. The two main tools of SPC are control charts and process capability analysis. The popular Shewhart $\overline{X}$ and R charts are extensively applied to graphically controlling the process mean and range variations [1].

On the other hand, the process capability indices are commonly used in process analysis to numerically exhibit how the process is performing relative to specification limits. Nevertheless, process capability evaluation and control charts implementation require data obtained through measurements. Since measurement system variability cannot be avoided [2], it must be taken into account before and while assessing process capability and calculating control charts limits. DR was developed to compare the former variability to the process unevenness and employed as a measurement system acceptability criterion [2–4].

The majority of research works related to control chart assumed that the used measurement system is perfect and free from errors. Therefore, control limits are calculated based on the total variability including the real process variability and the measurement system variability. In some cases, the real process state is much better than the observed one and the observed total variation is mainly governed, by the variability of the measurement system rather than the process. If this fact is not considered, unreliable decisions about the process may be made [5]. The purpose of this investigation is to contribute filling this gap of knowledge by developing $\overline{X}$ and R control charts limits for the real process state. The paper is divided into two major parts. In the first part, effects of the measurement system variability on the commonly used process capability indices, C_p and C_{pm} are discussed. In the second part, calculation methods for Shewhart $\overline{X}$, R control charts limits are developed to consider the real process state.

* Corresponding author: benfredjnabil@gmail.com

2 Impact of measurement system variability on process capability indices C_p and C_{pm}

2.1 Effects on the process capability index C_p

In the case of stable, normally distributed process, having two sided symmetric specification limits and the mean of the distribution is centred at the middle of the specifications, C_p is defined as below [6]:

$$C_p = \frac{\mathrm{USL} - \mathrm{LSL}}{6\sigma_p} = \frac{d}{3\sigma_p}, \tag{1}$$

where σ_p is the real process standard deviation, USL and LSL are the upper and lower specification limits, respectively and d is the half specification width ($d = (\mathrm{USL}-\mathrm{LSL})/2$). The index C_p measures the process ability to manufacture products that meet the specification limits.

Nevertheless, due to measurement system variability, the total observed variance (σ_t^2) cumulates variances of the process (σ_p^2) and the measurement system (σ_m^2):

$$\sigma_t{}^2 = \sigma_p{}^2 + \sigma_m{}^2. \tag{2}$$

Consequently, a usual problem tackled in practice consisting on how to distinguish between the measurement system and the process variabilities. Therefore, it is essential to assess the measurement system variability σ_m by conducting an analysis as recommended by the Automotive Industry Action Group (AIAG) standard [7]. This standard, defines the measurement system discrimination ratio (DR) as follows:

$$\mathrm{DR} = \sqrt{\frac{2\sigma_p{}^2}{\sigma_m{}^2} + 1}. \tag{3}$$

DR describes how many classifications can be reliably distinguished by the measurement system [7]. The value of DR is compared to a threshold value to make the appropriate decision about the measurement system acceptability. Wheeler and Lyday [8] stated that while DR more than 4 is acceptable, DR less than 2 indicates that the measurement system is inadequate to evaluate the process variability. When DR ranges between 2 and 4, the measurement system may be accepted for some specific applications.

As for the process capability evaluation, in practice, a capability analysis yields to an observed capability index ($C_{p,\mathrm{Obs}}$) integrating the total variability (σ_t) rather than the process true index ($C_{p,\mathrm{True}}$). $C_{p,\mathrm{Obs}}$ is expressed as follows:

$$C_{p,\mathrm{Obs}} = \frac{d}{3\sigma_t} = \frac{d}{3\sqrt{\sigma_p{}^2 + \sigma_m{}^2}}. \tag{4}$$

Consequently, the process true capability index $C_{p,\mathrm{True}}$ can be given as below:

$$C_{p,\mathrm{True}} = \sqrt{1 + \frac{\sigma_m{}^2}{\sigma_p{}^2}} C_{p,\mathrm{Obs}}. \tag{5}$$

Based on equation (3), $C_{p,\mathrm{True}}$ can be expressed as function of DR as:

$$C_{p,\mathrm{True}} = C_{p,\mathrm{Obs}} \sqrt{1 + \left(\frac{2}{\mathrm{DR}^2 - 1}\right)}. \tag{6}$$

Equation (6) shows that low values of DR result on wide differences between $C_{p,\mathrm{Obs}}$ and $C_{p,\mathrm{True}}$.

2.2 Effects on the process capability index C_{pm}

Taguchi [9] identified another source of process variability related to decentring. He stated that as the measured product characteristic (X) departs from a predefined target value (T) an economic loss is incurred. Hence, to express this loss, he proposed the following quadratic loss function [9]:

$$\mathrm{Loss}(X) = k(X - T)^2, \tag{7}$$

where k expresses the quality loss coefficient. This coefficient may be deduced from a replacement/repair cost function $A_0 = \mathrm{Loss}(T \pm d)$ pertaining to a nonconforming part and expressed as below [10,11],

$$\mathrm{Loss}(T \pm d) = A_0 = k((T \pm d) - T)^2. \tag{8}$$

Therefore,

$$k = \frac{A_0}{d^2}. \tag{9}$$

The expected mean value of the Taguchi loss function can be expressed as follow [10]:

$$E(\mathrm{Loss}) = k[\sigma_p^2 + (\mu - T)^2], \tag{10}$$

where (μ) is the process mean.

Based on this concept, Chan et al. [12] introduced the Taguchi capability index C_{pm} that is directly related to the former quadratic loss function of the measured feature. In the case of stable, normally distributed process, having two sided specification limits and a target value T that can be different from the process mean μ, C_{pm} is defined as below [12]:

$$C_{\mathrm{pm}} = \frac{\mathrm{USL} - \mathrm{LSL}}{6\sqrt{\sigma_p{}^2 + (\mu - T)^2}} = \frac{d}{3\sqrt{\sigma_p{}^2 + (\mu - T)^2}}. \tag{11}$$

The index C_{pm} emphasizes the ability of the process to cluster around the target. Hence, it takes into account both the process decentring and variability [13]. In practice, the measured index is denoted as the observed one $C_{\mathrm{pm,Obs}}$ and defined as:

$$C_{\mathrm{pm,Obs}} = \frac{\mathrm{Tol}}{6\sqrt{\sigma_t{}^2 + (\mu - T)^2}}. \tag{12}$$

While the true process capability index is denoted as $C_{\mathrm{pm,True}}$, the relationship between $C_{\mathrm{pm,Obs}}$ and $C_{\mathrm{pm,True}}$ can be given by the following expressions:

$$\begin{aligned}\frac{C_{\mathrm{pm,True}}}{C_{\mathrm{pm,Obs}}} &= \frac{\mathrm{Tol}/\left(6\sqrt{{\sigma_p}^2+(\mu-T)^2}\right)}{\mathrm{Tol}/\left(6\sqrt{{\sigma_t}^2+(\mu-T)^2}\right)} \\ &= \frac{\sqrt{\sigma_t^2+(\mu-T)^2}}{\sqrt{\sigma_p^2+(\mu-T)^2}} = \frac{\sqrt{(\sigma_m^2+\sigma_p^2)+(\mu-T)^2}}{\sqrt{\sigma_p^2+(\mu-T)^2}}. \\ &= \frac{\sqrt{1+(\sigma_m/\sigma_p)^2+((\mu-T)/\sigma_p)^2}}{\sqrt{1+((\mu-T)/\sigma_p)^2}}\end{aligned} \tag{13}$$

Equation (3) and equation (13) yield to the following relationship:

$$\begin{aligned}\frac{C_{\mathrm{pm,True}}}{C_{\mathrm{pm,Obs}}} &= \frac{\sqrt{1+(2/(\mathrm{DR}^2-1))+((\mu-T)/\sigma_p)^2}}{\sqrt{1+((\mu-T)/\sigma_p)^2}} \\ &= \sqrt{\frac{1+{A_1}^2+(2/(\mathrm{DR}^2-1))}{1+A_1 2}} \\ &= \sqrt{1+\frac{2}{(1+A_1^2)\times(\mathrm{DR}^2-1)}}\end{aligned}, \tag{14}$$

where

$$A_1 = \frac{|\mu-T|}{\sigma p},$$

A_1 is the ratio of the process decentering from target value T to its variation σ_p.

As σ_p is unknown, it can be deduced from the observed capability index $C_{p,\mathrm{Obs}}$ (Eq. (6)) as follow:

$$\begin{aligned}\sigma_p^2 &= \frac{\sigma_t^2}{(1+(\sigma_m^2/\sigma_p^2)} = \frac{\sigma_t^2}{1+(2/(\mathrm{DR}^2-1))} \\ &= \frac{d^2}{9\times(C_{p,\mathrm{Obs}})^2\times(1+(2/(\mathrm{DR}^2-1)))}.\end{aligned} \tag{15}$$

Process capability index $C_{\mathrm{pm,True}}$ can be used to draw conclusions about process fallouts expressed in expected non conforming units of ppm. In recent work, Perakis and Xekalaki [14] defined the proportion of conformance of a process (P) while neglecting the measurement system error ($C_{\mathrm{pm,Obs}} = C_{\mathrm{pm,True}}$) by the following expression:

$$\begin{aligned}P = &\phi\left(\frac{\mathrm{USL}-\mu}{\sqrt{\left(\frac{d}{3C_{\mathrm{pm,True}}}\right)^2-(\mu-T)^2}}\right) \\ &-\phi\left(\frac{\mathrm{LSL}-\mu}{\sqrt{\left(\frac{d}{3C_{\mathrm{pm,True}}}\right)^2-(\mu-T)^2}}\right).\end{aligned} \tag{16}$$

Hence, the ppm can be written as follows:

$$\begin{aligned}\mathrm{ppm} = 10^6 \times \Bigg[1-\Bigg(&\phi\left(\frac{\mathrm{USL}-\mu}{\sqrt{\left(\frac{d}{3C_{\mathrm{pm,True}}}\right)^2-(\mu-T)^2}}\right) \\ &-\phi\left(\frac{\mathrm{LSL}-\mu}{\sqrt{\left(\frac{d}{3C_{\mathrm{pm,True}}}\right)^2-(\mu-T)^2}}\right)\Bigg)\Bigg],\end{aligned} \tag{17}$$

where $\phi(\cdot)$ denotes the standard normal cumulative distribution function.

However, as indicated above, the measurement system error cannot be neglected and equation (17) will be corrected in the followings to consider the impact of the measurement system variability on ppm.

$$\begin{aligned}\mathrm{ppm} = 10^6 &\times\Bigg[1-\Bigg(\phi\left(\frac{\mathrm{USL}-\mu}{\sqrt{\left(\frac{d}{3C_{\mathrm{pm,Obs}}\sqrt{1+\frac{2}{(1+A_1{}^2)\times(\mathrm{DR}^2-1)}}}\right)^2-(\mu-T)^2}}\right) \\ &-\phi\left(\frac{\mathrm{LSL}-\mu}{\sqrt{\left(\frac{d}{3C_{\mathrm{pm,Obs}}\sqrt{1+\frac{2}{(1+A_1{}^2)\times(\mathrm{DR}^2-1)}}}\right)^2-(\mu-T)^2}}\right)\Bigg)\Bigg].\end{aligned} \tag{18}$$

In order to highlight the effects of the measurement system variability on ppm, the same example used in reference [15] (see Appendix) and initially employed by Grant and Leavenworth [16] is utilized to compute ppm for different values of DR (Tab. 1). Data are pertaining to measurements of diameters on shafts. In this paper, as international unit system is used, data of reference [15] that are originally in inch were converted in mm. The lower and the upper specification limits are set to 10.22 mm (0.4024 in) and 10.28 mm (0.4050 in) respectively, and target value is assumed to be equal to 10.248 mm (0.4035 in) and the process mean is equal to 10.245 mm (0.403355 in). The observed process capability indices calculated using the data set are $C_{p,\mathrm{Obs}} = 1.228$ and $C_{\mathrm{pm,Obs}} = 1.135$ (Eqs. (4) and (12)). If measurement error is neglected then equation (17) can be used to compute ppm. The calculated value in this case is ppm = 3415 units (Tab. 1).

As shown in Table 1, increasing the measurement system DR suggests that the process capability is evaluated with a measurement system with lower variability. Therefore, the total variation tends to be equal to the

Table 1. Values of $C_{pm,True}$ function of DR with associated values of expected ppm.

$C_{pm,Obs}$	ppm ($C_{pm,Obs}$)	DR	$C_{pm,True}$	ppm ($C_{pm,True}$)
		2	1.400	239
		2.5	1.299	739
		3	1.247	1245
		4	1.197	1989
1.135	3415	5	1.175	2434
		6	1.163	2707
		7	1.155	2882
		8	1.151	3001
		9	1.147	3084

Table 2. Values of $C_{pm,Obs}$ and $C_{pm,True}$ with associated values of E(Loss)\$.

$C_{pm,Obs}$	E(Loss)\$ ($C_{pm,Obs}$)	DR	$C_{pm,True}$	E(Loss)\$ ($C_{pm,True}$)
		2	1.400	3846
		2.5	1.299	4145
		3	1.247	4317
		4	1.197	4497
1.135	4742	5	1.175	4583
		6	1.163	4631
		7	1.155	4660
		8	1.151	4679
		9	1.147	4692

process variation. Hence, $C_{pm,Obs}$ becomes closer to $C_{pm,True}$ and consequently, the gap between the expected ppm calculated using the observed $C_{pm,Obs}$ and using $C_{pm,True}$ becomes much narrow. It is important to notice that the expected ppm when using a measurement system with a DR = 4 (value recommended by the AIAG) is equal to 1989. In this case, the expected ppm is overestimated to about 41% of it is real value.

The economic consequences of this overestimation affect directly the expected loss that can be expressed as function of $C_{pm,True}$ by referring to equations (10) and (11) as below:

$$E(\text{Loss}) = \frac{kd^2}{9C_{pm,True}}. \tag{19}$$

Based on data of the example introduced earlier, E(Loss) is firstly calculated while neglecting measurement variability ($C_{pm,True} = C_{pm,Obs}$) and secondly when considering this variability for different values of DR. The replacement/repair cost A_0 is supposed to be equal to 40×10^3\$, hence the quality loss coefficient k[\$/mm^2] is equal to 44.44×10^6\$/mm^2 [15]. Results are summarized in Table 2.

From Table 2, it can be observed that E(Loss) becomes higher as DR increases. This can be explained by the fact that measurement variability overlaps the real variability of the process. Indeed, by using a measurement system with smaller DR, practitioner assesses observed process capability that is lower than the true one and E(Loss) value is underestimated in this case.

3 $\overline{X}$ and R control charts limits calculation with measurement system variability consideration

When the controlled quality characteristic is a variable, $\overline{X}$ and R control charts are commonly used. These charts are constructed from data collected by sampling. While $\overline{X}$ control chart is used for monitoring the process mean, R chart is used to supervise the process variability.

Control limits for the $\overline{X}$ chart are formulated as below [1]:

$$UCL_{\overline{X}} = \overline{\overline{X}} + 3\sigma_{\overline{X}_p}, \tag{20}$$

$$\text{LCL}_{\overline{X}} = \overline{\overline{X}} - 3\sigma_{\overline{X}_p}, \tag{21}$$

where $\overline{\overline{X}}$ is the process mean and $\sigma_{\overline{X}_p}$ is the standard deviation of $\overline{X}_{i,i=1,\ldots,m}$ (m number of samples) without considering the measurement variability.

The observed $\sigma_{\overline{X}_t}$ that takes into account the measurement variability can be deduced from the total observed variability:

$$\sigma_{\overline{X}_t} = \frac{\sigma_t}{\sqrt{n}} = \frac{\sqrt{\sigma_p{}^2 + \sigma_m{}^2}}{\sqrt{n}}. \tag{22}$$

On the other hand, $\sigma_{\overline{X}_p}$ can be expressed as follows:

$$\sigma_{\overline{X}_p} = \frac{\sigma_p}{\sqrt{n}}. \tag{23}$$

By referring to equation (6), $\sigma_{\overline{X}_p}$ can be given as:

$$\sigma_{\overline{X}_p} = \frac{d}{3\sqrt{n}C_{p,True}} = \frac{d}{3C_{p,Obs}\sqrt{n(1 + (2/(\text{DR}^2 - 1)))}}. \tag{24}$$

In the followings, the effect of the discrimination ratio DR on the control chart limits calculation will be discussed under the main condition of fixed value of $C_{p,Obs}$ (*i.e.* $C_{p,Obs} = 1.22$).

Figure 1 shows the relationship between the discrimination ratio DR and the normalized ratio ($\sigma_{\overline{X}_p}/d$) for different sample sizes n. This figure clearly shows that the effect of DR is widely conditioned by the sample size. Indeed, the measurement system variability evaluated by DR has no significant effect on the normalized ratio

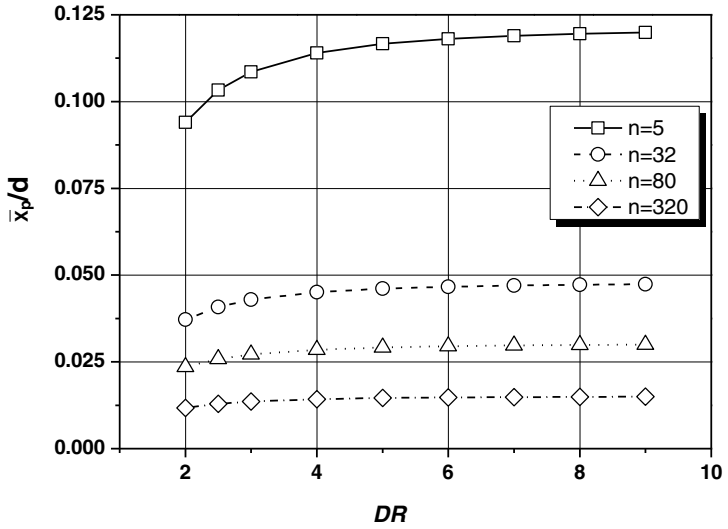

Fig. 1. Relationship between DR and the ratio $(\sigma_{\overline{X}_p}/d)$ ($C_{p,\mathrm{Obs}} = 1.22$).

$(\sigma_{\overline{X}_p}/d)$ for high values of the sample size (i.e. $n = 320$). In these cases, no particular correction is required for control charts limits. Meanwhile, for small sample size corrections must be carried out to take into account the variability of the measurement system. According to plots of Figure 1, the recommended value of DR by the AIAG (DR = 4), seems to be an acceptable threshold value from which the measurement system can be applied in SPC.

Moreover, this figure shows that even measurement systems with DR lower than the recommended threshold value, that are unacceptable according to AIAG standard, can be used to control and monitor the process after introducing the required corrections to chart limits.

These corrections can be expressed as below.

For $\overline{X}$ *chart:* based on equations (20), (21) and (24), chart properties can be given as follows:

$$\text{The centerline: } \mathrm{CL}_{\overline{X}} = \overline{\overline{X}}. \tag{25}$$

$$\text{The upper control limit: } \mathrm{UCL}_{\overline{X}} = \overline{\overline{X}} + \frac{d}{C_{p,\mathrm{Obs}}\sqrt{n \times \left[\frac{2}{\mathrm{DR}^2-1}+1\right]}}. \tag{26}$$

$$\text{The lower control limit: } \mathrm{LCL}_{\overline{X}} = \overline{\overline{X}} - \frac{d}{C_{p,\mathrm{Obs}}\sqrt{n \times \left[\frac{2}{\mathrm{DR}^2-1}+1\right]}}. \tag{27}$$

For the R *chart:*

The samples average range $\overline{R}$ can be expressed as function of the estimated process standard deviation as [1]:

$$\overline{R} = d_2\hat{\sigma}_p, \tag{28}$$

where d_2 is a constant that depends on the sample size [1].

The estimated process standard deviation $\hat{\sigma}_p$ can be calculated as follows:

$$\sigma_{\overline{X}_p} = \frac{\hat{\sigma}_p}{\sqrt{n}}. \tag{29}$$

Therefore,

$$\overline{R} = d_2\sqrt{n}\sigma_{\overline{X}_p}. \tag{30}$$

By referring to the equation (24), the average range can be expressed as:

$$\overline{R} = \frac{dd_2}{3C_{p,\mathrm{Obs}}\sqrt{\left[\frac{2}{\mathrm{DR}^2-1}+1\right]}}. \tag{31}$$

Figure 2 shows the variation of samples average range $\overline{R}$ as function of DR for fixed value of $C_{p,\mathrm{Obs}}$ (*i.e.* $C_{p,\mathrm{Obs}} = 1.22$). This figure shows that similarly to the $\overline{X}$ chart, the samples average range $\overline{R}$ is dependent on the sample size and the measurement system discrimination ratio DR has a significant effect on the $\overline{R}$ chart characteristics. This effect is seen to be as important as DR is low.

Here also, measurement systems with low DR can be used for monitoring the process variation after introducing the corrections below:

$$\text{The center line: } \mathrm{CL}_R = \frac{d\,d_2}{3C_{p,\mathrm{Obs}}\sqrt{\left[\frac{2}{\mathrm{DR}^2-1}+1\right]}}. \tag{32}$$

$$\text{The upper control limit: } \mathrm{UCL}_R = D_4\frac{d\,d_2}{3C_{p,\mathrm{Obs}}\sqrt{\left[\frac{2}{\mathrm{DR}^2-1}+1\right]}}. \tag{33}$$

$$\text{The lower control limit: } \mathrm{LCL}_R = D_3\frac{d\,d_2}{3C_{p,\mathrm{Obs}}\sqrt{\left[\frac{2}{\mathrm{DR}^2-1}+1\right]}}. \tag{34}$$

Constants D_4 and D_3 depend on sample size n [1].

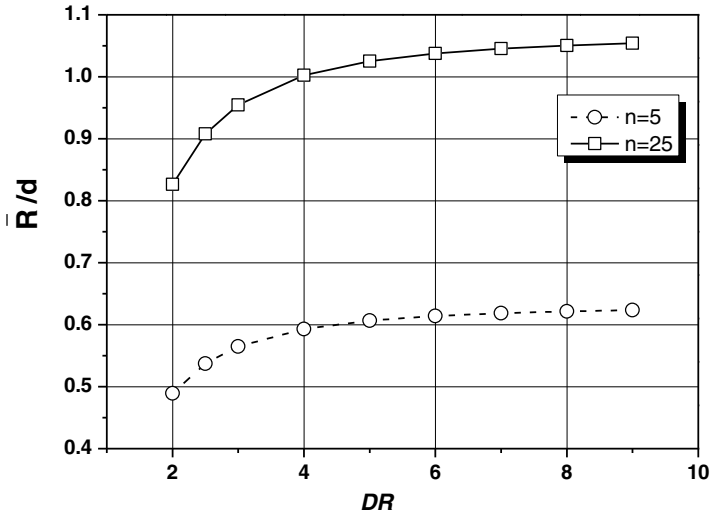

Fig. 2. Variation of $\overline{R}$ depending on DR ($C_{p,\mathrm{Obs}} = 1.22$).

Table 3. Comparison between traditional and corrected control limits for different values of DR ($C_{\mathrm{p,Obs}} = 1.22$).

	Traditional control limits ($\sigma_{\overline{X}_p} = \sigma_{\overline{X}_t}$)	Corrected control limits ($\sigma_{\overline{X}_p} \neq \sigma_{\overline{X}_t}$)		
		DR = 2	DR = 4	DR = 9
$\mathrm{CL}_{\overline{X}}$	10.2452	10.2452	10.2452	10.2452
$\mathrm{UCL}_{\overline{X}}$	10.2572	10.2545	10.2565	10.2570
$\mathrm{LCL}_{\overline{X}}$	10.2332	10.2359	10.2339	10.2333
CL_R	0.02085	0.0161	0.0196	0.0206
UCL_R	0.0441	0.0341	0.0414	0.0435
LCL_R	0	0	0	0

4 Illustrative example

The machined shafts example described earlier is used to put in evidence the importance of the proposed corrections that must be made for control charts limits calculation depending on the measurement system discrimination ratio *DR*. In this example, sampling is made using a sample size $n = 5$. Therefore, $d_2 = 2.326$, $D_3 = 0$ and $D_4 = 2.114$ (for details see reference [1]).

Results of limits calculations are given in Table 3 for DR = 2, 4 and 9. In this table, the traditional control limits refer to limits calculation under the assumption of perfect measurement system ($\sigma_{\overline{X}_t} \approx \sigma_{\overline{X}_p}$).

Corrected control limits in cases of DR = 2, 4 and 9 and uncorrected control limits are plotted in Figure 3a and b for $\overline{X}$ and R control chart, respectively. In Figure 3a, in order to reduce the scale effect between a sample mean ($\overline{X}_i$, in the order of 10.2xx mm) and the difference between two means ($(\overline{X}_i - \overline{X}_j)$, in the order of 0.0xx mm), $\overline{X}$ chart is plotted using $(\overline{X}_i - 10.200)$ mm format.

Control charts given by Figure 3 show that the widest upper and lower control limits correspond to the traditional ones followed by limits calculated for DR = 9 and thereafter DR = 4. This is because uncorrected limits consider both process and measurement system variabilities. For a constant value of observed capability, the contribution of the measurement system on the total observed variability increases for low values of DR. This means that the observed variability is governed by the measurement system rather than the process variability. Therefore, control charts parameters must be corrected to avoid misinterpretation of the process state and the consequent wrong decisions.

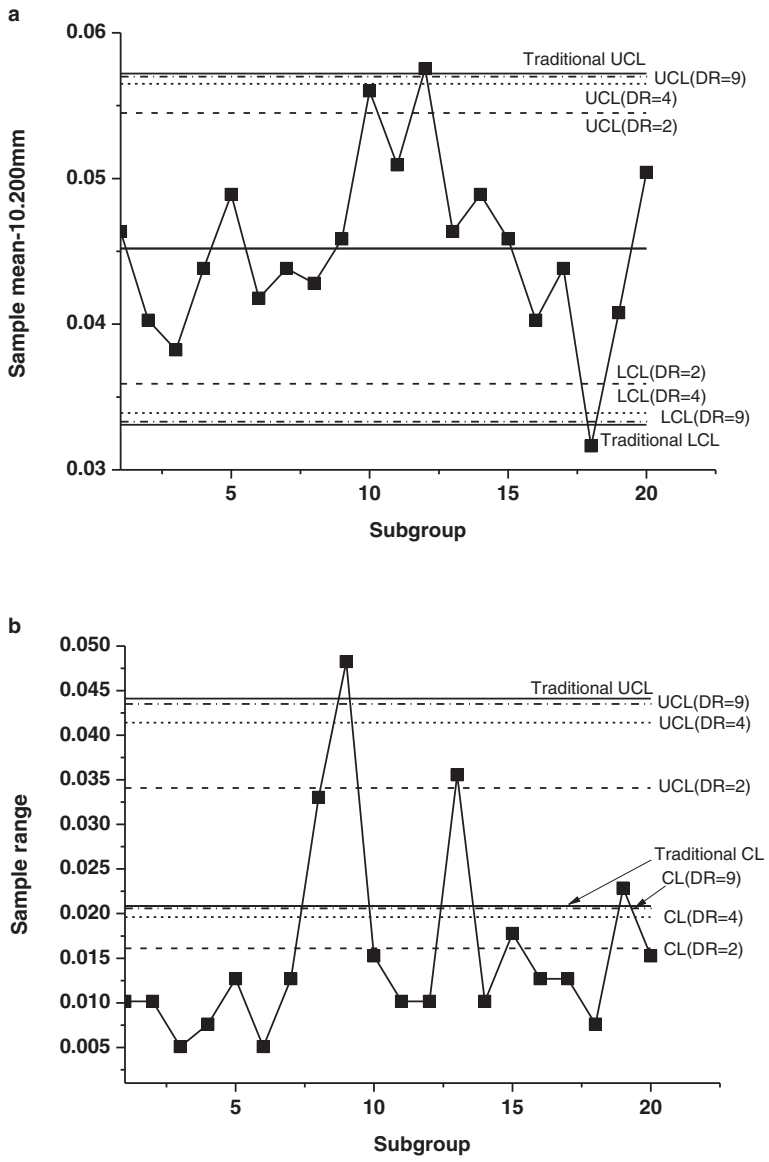

Fig. 3. ($\overline{X}$, R) Shewhart charts plotted using corrected (DR = 2, 4 and 9) and traditional limits. (a) $\overline{X}$ chart, (b) R chart.

5 Conclusion

The work presented in this paper deals with issue related to the effects of measurement system variability evaluated by the discrimination ratio DR on the process capability indices $C_p$and C_{pm}, on the expected non conforming units of ppm, on the expected mean value of the Taguchi loss function (E(Loss)) and on the Shewhart $\overline{X}$ and R charts properties. It was found that DR has significant effects on these process characterization parameters and that the accurate calculation of these parameters must consider the measurement system variability. Therefore, new equations were developed to integrate these effects. When exploring these equations, it was found that differences between the observed uncorrected parameters and the corrected ones are as significant as the discrimination ratio DR is low.

5.1 Implication and influences

Process capability indices and control charts are appropriate tools to evaluate process performances and monitor its outputs. However, quality practitioner may not pay attention to measurement system variability when evaluating and controlling the process. This paper shows that the measurement system variability has a significant impact on the calculation of the capability indices C_p and C_{pm}, on the expected non conforming units of ppm, on the expected mean value of the Taguchi loss function E(Loss) and on the control charts parameters. For this purpose, new calculation methods to evaluate the real process state were developed to help avoiding wrong analysis and the consequent unreliable decisions.

Appendix. Measured diameters on turned shafts (mm) [15].

Sample number	Measurements					Sample mean (mm)	Sample range R (mm)
1	10.251	10.249	10.246	10.244	10.241	10.246	0.0102
2	10.239	10.239	10.246	10.241	10.236	10.240	0.0102
3	10.236	10.236	10.241	10.236	10.241	10.238	0.0051
4	10.241	10.244	10.244	10.241	10.249	10.244	0.0076
5	10.241	10.246	10.254	10.254	10.249	10.249	0.0127
6	10.241	10.241	10.239	10.244	10.244	10.242	0.0051
7	10.244	10.244	10.251	10.241	10.239	10.244	0.0127
8	10.218	10.244	10.251	10.249	10.251	10.243	0.0330
9	10.269	10.251	10.249	10.221	10.239	10.246	0.0483
10	10.251	10.249	10.251	10.264	10.264	10.256	0.0152
11	10.246	10.257	10.249	10.246	10.257	10.251	0.0102
12	10.251	10.257	10.259	10.259	10.262	10.258	0.0102
13	10.251	10.262	10.249	10.226	10.244	10.246	0.0356
14	10.251	10.249	10.254	10.246	10.244	10.249	0.0102
15	10.236	10.254	10.244	10.246	10.249	10.246	0.0178
16	10.231	10.239	10.244	10.244	10.244	10.240	0.0127
17	10.244	10.236	10.246	10.244	10.249	10.244	0.0127
18	10.229	10.231	10.234	10.229	10.236	10.232	0.0076
19	10.249	10.251	10.234	10.229	10.241	10.241	0.0229
20	10.244	10.249	10.249	10.259	10.251	10.250	0.0152

References

1. D.C. Montgomery, *Statistical Quality Control: A Modern Introduction* (Wiley, New York, 2009), 6th ed.
2. A. Al-Refaie, N. Bata, Evaluating measurement and process capabilities by *GR&R* with four quality measures, Measurement **43**, 842–851 (2010)
3. G. Knowles, G. Vickers, J. Anthony, Implementing evaluation of the measurement process in an automotive manufacturer: a case study, Qual. Reliab. Eng. Int. **19**, 397–410 (2003)
4. D.P. Mader, J. Prins, R.E. Lampe, The economic impact of measurement error, Qual. Eng. **11**, 563–574 (1999)
5. W.L. Pearn, S. Kotz, *Encyclopedia and Handbook of Process Capability Indices—Series on Quality. Reliability and Engineering Statistics* (World Scientific, Singapore, 2007)
6. V.E. Kane, Process capability indices, J. Qual. Technol. **18**, 41–52 (1986)
7. AIAG: Automotive Industry Action Group, *Measurement Systems Analysis Reference Manual* (Chrysler Corporation, Ford Motor Company, General Motors Corporation, Detroit, MI, 2010), 4th ed.
8. D.J. Wheeler, R.W. Lyday, *Evaluating the Measurement Process* (SPC Press Inc., Knoxville, TN, 1989), 2nd ed.
9. G. Taguchi, *Introduction to Quality Engineering, Designing Quality into Products and Processes* (Asian Productivity Organization, Tokyo, 1988)
10. G. Celano, A. Faraz, E. Saniga, Control charts monitoring product's loss to society, Qual. Reliab. Eng. Int. **30**, 1393–1407 (2014)
11. F. Amiri, K. Noghondarian, A.S. Safaei, Evaluating the performance of variable scheme X-bar control chart: a Taguchi loss approach, Int. J. Prod. Res. **52**, 5385–5395 (2014)
12. L.K. Chan, S.W. Cheng, F.A. Spiring, A new measure of process capability: C_{pm}, J. Qual. Technol. **20**, 162–175 (1988)
13. M. Pillet, S. Rochon, E. Duclos, SPC-Generalization of capability index C_{pm}: case of unilateral tolerances, Qual. Eng. **10**, 171–176 (1997)
14. M. Perakis, E. Xekalaki, On the relationship between process capability indices and the proportion of conformance, Qual. Technol. Quant. Manag. **13**, 207–220 (2016), doi:10.1080/16843703.2016. 1169696
15. D.G. Sauers, Using the Taguchi loss function to reduce common-cause variation, Qual. Eng. **12**, 245–252 (1999)
16. E.L. Grant, R.S. Leavenworth, *Statistical Process Control* (McGraw-Hill, New York, 1980), 5th ed.

Cite this article as: Souha Ben Amara, Jamel Dhahri, Nabil Ben Fredj, Control chart limits based on true process capability with consideration of measurement system error, Int. J. Metrol. Qual. Eng. **7**, 401 (2016)